

1 **C2CD6 is required for assembly of the CatSper calcium channel complex and**  
2 **fertilization**

3

4 **Fang Yang<sup>1,5</sup>, Maria Gracia Gervasi<sup>2,5</sup>, N. Adrian Leu<sup>1</sup>, Darya A. Tourzani<sup>2,3</sup>, Gordon Ruthel<sup>4</sup>,**  
5 **Pablo E. Visconti<sup>2</sup>, P. Jeremy Wang<sup>1</sup>**

6

7 <sup>1</sup>Department of Biomedical Sciences, University of Pennsylvania School of Veterinary Medicine,  
8 Philadelphia, PA 19104, USA.

9 <sup>2</sup>Department of Veterinary and Animal Sciences, University of Massachusetts, Amherst, MA 01003,  
10 USA.

11 <sup>3</sup>Biotech Training Program (BTP), Animal Biotechnology and Biomedical Sciences Graduate Program,  
12 Department of Veterinary and Animal Sciences. University of Massachusetts, Amherst, MA 01003,  
13 USA.

14 <sup>4</sup>Department of Pathobiology, University of Pennsylvania School of Veterinary Medicine,  
15 Philadelphia, PA 19104, USA.

16 <sup>5</sup>These authors contributed equally.

17

18 Author for correspondence (email: [pwang@vet.upenn.edu](mailto:pwang@vet.upenn.edu)).

19

20

21

22

23

## 24 **Summary**

25 The CatSper cation channel is essential for sperm capacitation and male fertility. The multi-subunit  
26 CatSper complexes form highly organized calcium signaling nanodomains on flagellar membranes.  
27 Here we report identification of an uncharacterized protein C2CD6 as a novel subunit of the CatSper  
28 ion channel complex. C2CD6 contains a calcium-dependent membrane targeting C2 domain. C2CD6  
29 interacts with the CatSper calcium-selective core forming subunits. Deficiency of C2CD6 depletes the  
30 CatSper nanodomains from the flagellum and results in male sterility. C2CD6-deficient sperm are  
31 defective in hyperactivation and fail to fertilize oocytes both in vitro and in vivo. Interestingly,  
32 transient treatments with either Ca<sup>2+</sup> ionophore, starvation, or a combination of both restore the  
33 fertilization capacity of C2CD6-deficient sperm in vitro. C2CD6 interacts with EFCAB9, a pH-  
34 dependent calcium sensor in the CatSper complex. We postulate that C2CD6 may regulate CatSper  
35 assembly, target the CatSper complex to flagellar plasma membrane, and function as a calcium sensor.  
36 The identification of C2CD6 as an essential subunit may facilitate the long-sought reconstitution of the  
37 CatSper ion channel complex in a heterologous system for male contraceptive development.

38

## 39 **Introduction**

40 Sperm acquires fertilization competence in the female reproductive tract (Chang, 1951). Sperm  
41 hyperactivated motility triggered by capacitation is essential for navigation in the oviduct (Suarez,  
42 2016), rheotaxis (Miki and Clapham, 2013), and zona pellucida penetration (Stauss et al., 1995). The  
43 uterus and oviduct fluids provide an alkaline environment and a high concentration of bicarbonate,  
44 which are critical for capacitation (Vishwakarma, 1962). Sperm motility is regulated by ion channels  
45 and ion transporters in the flagellum in response to environmental stimuli (Vylicka and Lishko,  
46 2020). Calcium influx in sperm is gated by the CatSper ion channel in the flagellum (Ren et al., 2001).  
47 The CatSper channel is activated by alkaline pH in rodents (Kirichok et al., 2006) and primates  
48 (Lishko et al., 2010), and by progesterone (P4) in primates (Lishko et al., 2011; Strunker et al., 2011).  
49 The CatSper channel forms four linear columns of Ca<sup>2+</sup> signaling domains along the principal piece of  
50 the sperm flagellum (Chung et al., 2014). The CatSper domains organize the spatiotemporal pattern of  
51 tyrosine phosphorylation of flagellar proteins, one of the hallmarks of capacitation (Chung et al.,  
52 2014; Visconti, P. E. et al., 1995). Calcium influx caused by the CatSper activation results in powerful  
53 asymmetrical flagellar beating movement known as hyperactivation. CatSper is inhibited by efflux of  
54 potassium, which is carried out by the Slo3 K<sup>+</sup> channel (Brenker et al., 2014; Chavez et al., 2014; Geng  
55 et al., 2017; Santi et al., 2010; Schreiber et al., 1998; Zeng et al., 2011). In human spermatozoa, P4 binds  
56 to its sperm membrane receptor ABHD2, which hydrolyzes the endocannabinoid 2-

57 arachidonoylglycerol (2-AG), an inhibitor of the CatSper channel. As a result, P4 activates CatSper by  
58 removing 2-AG from the plasma membrane (Miller et al., 2016). Therefore, sperm hyperactivation is  
59 regulated by both environmental stimuli in the female reproductive tract and ion channels on sperm  
60 flagella.

61 The CatSper channel is a complex of ten known subunits: CatSper1-4, CatSper $\beta$ ,  $\gamma$ ,  $\delta$ ,  $\epsilon$ ,  $\zeta$ , and  
62 EFCAB9 (Lin et al., 2021;Vyklicka and Lishko, 2020;Wang et al., 2021). CatSper1-4 subunits form a  
63 heteromeric complex with a central Ca<sup>2+</sup>-selective pore. The remaining six subunits are auxiliary  
64 proteins. While CatSper $\beta$ ,  $\gamma$ ,  $\delta$ , and  $\epsilon$  are putative transmembrane proteins, CatSper $\zeta$  and EFCAB9 lack  
65 transmembrane domains (Chung et al., 2011;Chung et al., 2017;Hwang et al., 2019;Liu et al.,  
66 2007;Wang et al., 2009). Genetic ablation in mice and humans have revealed the role of the CatSper  
67 subunits in male fertility. Each of the CatSper core subunits (CatSper1-4) is required for the CatSper  
68 complex formation, sperm hyperactivation, and thus, for male fertility (Carlson et al., 2003;Carlson et  
69 al., 2005;Jin et al., 2007;Qi et al., 2007;Quill et al., 2003;Ren et al., 2001). Like CatSper1-4, CatSper $\delta$ ,  
70 is essential for CatSper channel complex assembly and male fertility (Chung et al., 2011). In contrast,  
71 CatSper $\zeta$  or EFCAB9-deficient males exhibit subfertility (Chung et al., 2017;Hwang et al., 2019). In  
72 CatSper $\zeta$  or EFCAB9-deficient mouse mutants, the CatSper Ca<sup>2+</sup> signaling domain organization is  
73 affected but the CatSper channel is still functional. EFCAB9 is an EF-hand calcium binding protein.  
74 EFCAB9 interacts with CatSper $\zeta$  and this interaction requires the binding of Ca<sup>2+</sup> to EF-hand domains.  
75 Thus, EFCAB9 in partner with CatSper $\zeta$  functions as an intracellular pH dependent Ca<sup>2+</sup> sensor and  
76 activator for the CatSper channel (Hwang et al., 2019). Each of the four columns of CatSper domains  
77 consists of two rows. However, in CatSper $\zeta$  or EFCAB9-deficient mouse sperm, each column contains  
78 only one row of CatSper domains instead of two, suggesting a structural role in addition to their Ca<sup>2+</sup>  
79 sensor function. The CatSper channel is essential for male fertility in humans. Men with loss of  
80 function mutations in CatSper subunits are infertile due to failures in sperm hyperactivation (Avenarius  
81 et al., 2009;Brown et al., 2018;Luo et al., 2019;Smith et al., 2013).

82 CatSper is probably the most complex ion channel known to date. Despite the extensive  
83 genetic, super-resolution structural, and electrophysiological studies, a functional CatSper complex has  
84 not been reconstituted in a heterologous system. One possibility is that additional subunits are yet to be  
85 identified. Serendipitously, we identified a calcium-binding C2 membrane domain protein (C2CD6) as  
86 a novel subunit for the CatSper channel complex. Here, we demonstrate that C2CD6, like CatSper1-4  
87 and CatSper $\delta$ , is essential for the CatSper assembly, sperm hyperactivation, and male fertility.

88

## 89 **Materials and Methods**

90

### 91 **Generation of *C2cd6* knockout mice**

92 The targeting strategy was to delete 1.6-kb genomic region including exon 1 of the *C2cd6* gene (Fig.  
93 2A). In the targeting construct, the left (2.3 kb) and right (2.1 kb) homologous arms were PCR  
94 amplified from a *C2cd6*-containing mouse BAC clone (RP24-535E21) with high-fidelity Taq DNA  
95 polymerase. A neomycin (PGKNeo) selection marker was inserted between the homologous arms. The  
96 HyTK selection marker was cloned adjacent to the right arm. V6.5 embryonic stem (ES) cells were  
97 electroporated with the ClaI-linearized targeting construct and cultured in the presence of 350 µg/ml  
98 G418 and 2 µM ganciclovir. ES cell clones were screened by long-distance PCR for homologous  
99 recombination. Out of 192 ES cell clones, 9 homologously targeted clones were identified. 2C5 and  
100 1H1 ES cell clones were injected into blastocysts and the resulting chimeric mice transmitted the  
101 *C2cd6* knockout allele through the germline. The *C2cd6*<sup>+/-</sup> 2C5 mice were backcrossed to the  
102 C57BL/6J strain four times (N4). All the experiments were performed on the C57BL/6J N4  
103 backcrossed mice. Mice were genotyped by PCR of tail genomic DNA with the following primers:  
104 wild type (515 bp), ALS-25 (5'-GTATTTCCCATCATGTGGAGGA-3') and ALS-26 (5'-  
105 AGTGGCTTGCCTTCTTCATCAG-3'); *C2cd6* knockout allele (341 bp), ALS-9 (5'-  
106 TGTGCTATCCACCTTGCCTT-3') and PGKRNrev2 (5'-CCTACCGGTGGATGTGGAATGTGTG-  
107 3').

108 *CatSper1* knockout mice were previously generated (Ren et al., 2001). All experiments with  
109 mice were performed in accordance with the Institutional Animal Care and Use Committee (IACUC)  
110 guidelines of the University of Pennsylvania and the University of Massachusetts at Amherst.

111

### 112 **Antibody production**

113 The *C2cd6* cDNA was amplified from bulk mouse testis cDNA by PCR. The cDNA fragment  
114 encoding residues 1-386 was cloned into the pQE-30 vector (QIAGEN). The 6×His-C2CD6 (aa 1-386)  
115 fusion protein was expressed in M15 bacteria, affinity purified with Ni-NTA beads, and eluted in 8 M  
116 urea. The recombinant fusion protein was used to immunize two rabbits at Cocalico Biologicals, Inc.  
117 The C2CD6 antiserum (UP2429 and UP2430) was used for Western blotting analysis (1:500). Specific  
118 antibodies for immunofluorescence were affinity purified with the immunoblot method (Harlow and  
119 Lane, 1998).

120 The *Als2cr11b* cDNA fragment encoding the C-terminal 200 residues was cloned into the pQE-  
121 30 vector. The 6× His-ALS2CR11B (C-terminal 200 aa) fusion protein was expressed in bacteria,  
122 affinity purified, and used to immunize two rabbits at Cocalico Biologicals, In, resulting in one anti-  
123 ALS2CR11B antiserum (UP2443).

124

### 125 **In vivo fertilization**

126 Eight-week-old wild type C57BL/6 females were injected with 7.5 IU of PMSG, then with 7.5 IU of  
127 hCG 46 hours later, and mated with either *C2cd6<sup>+/-</sup>* or *C2cd6<sup>-/-</sup>* males. Copulatory plugs were checked  
128 17 hours after mating setup. 24 hours after plug check, eggs/embryos were flushed from plugged  
129 females. The numbers of two-cell embryos and one-cell embryos/eggs were counted.

130

### 131 **Sperm collection**

132 Cauda epididymides from three month-old males were dissected and placed in Toyoda-Yokoyama-  
133 Hosi (TYH) buffer containing 119.37 mM NaCl, 4.7 mM KCl, 1.71 mM CaCl<sub>2</sub>, 1.2 mM KH<sub>2</sub>PO<sub>4</sub>, 1.2  
134 mM MgSO<sub>4</sub>, 25.1 mM NaHCO<sub>3</sub>, 0.51 mM sodium pyruvate, 5.56 mM glucose, 4 mg/ml BSA, 10  
135 µg/ml gentamicin and 0.0006% phenol red equilibrated in 5% CO<sub>2</sub> at 37°C. After 10 minutes of sperm  
136 swim-out, epididymal tissue was removed and sperm suspensions were further incubated in TYH in  
137 5% CO<sub>2</sub> at 37 °C to allow sperm to capacitate.

138

### 139 **Sperm motility analysis**

140 Sperm motility parameters were analyzed immediately after swim-out (T0) and after 60 minutes (T60)  
141 of incubation in capacitating conditions (TYH medium). Sperm suspensions were loaded onto 100 µm  
142 depth chamber slides (Leja, Spectrum Technologies, CA), placed in a slide warmer at 37 °C  
143 (Minitherm, Hamilton Thorne), and imaged with a 4× dark field objective (Olympus) in a Lab A1  
144 microscope (Zeiss). Ninety frame videos were recorded at 60 Hz and analyzed using a CEROS II  
145 computer assisted sperm analysis system (Hamilton-Thorne Inc., Beverly, MA). The settings for cell  
146 recognition included: head size, 5-200; min head brightness, 100; and static head elongation, 5–100 %.  
147 Sperm with average path velocity (VAP) > 0 and rectilinear velocity (VSL) > 0 were considered  
148 motile. Sperm were considered progressive with VAP > 50 µm/s and straightness (STR) > 50 %, and  
149 hyperactive with curvilinear velocity (VCL) > 271 µm/s, VSL/VCL (LIN) < 50 %, and amplitude of  
150 lateral head displacement (ALH) > 3.5 µm. At least five fields per treatment corresponding to a  
151 minimum of 200 sperm were analyzed per experiment. Data were presented as percentage of motile

152 sperm out of the total population, and percentage of progressive or hyperactive sperm out of the motile  
153 population.

154

### 155 **In vitro fertilization (IVF)**

156 Young (7-9 weeks-old) CD-1 females were obtained from Charles River Laboratories (Wilmington,  
157 MA). Superovulation was induced by injection first with 7.5 IU of PMSG (Cat. No. 493-10, Lee  
158 Biosolution), followed 48 hours later with 7.5 IU of hCG (Cat. No. CG5, Sigma). Females were  
159 sacrificed 13 hours post-hCG injection, the oviducts were dissected, and cumulus-oocyte complexes  
160 (COCs) were collected in TL-HEPES medium containing 114 mM NaCl, 3.22 mM KCl, 2.04 mM  
161 CaCl<sub>2</sub>, 0.35 mM NaH<sub>2</sub>PO<sub>4</sub>, 0.49 mM MgCl<sub>2</sub>, 2.02 mM NaHCO<sub>3</sub>, 10 mM lactic acid (sodium salt), and  
162 10.1 mM HEPES. COCs were thoroughly washed with TYH and placed in an insemination drop of  
163 TYH covered by mineral oil previously equilibrated in an incubator in 5% CO<sub>2</sub> at 37 °C. COCs (2-3  
164 per 90 µl drop) were inseminated with 100,000 sperm that were previously capacitated in TYH  
165 medium for 60 minutes, and then were maintained in an incubator in 5% CO<sub>2</sub> at 37°C. After 4 hours of  
166 insemination, the MII-oocytes were washed, placed in a different drop of TYH media, and incubated  
167 overnight in 5% CO<sub>2</sub> at 37 °C. Dishes were examined 24 hours post-insemination and fertilization was  
168 evaluated by the appearance of two-cell stage embryos. Results were expressed as percentage of 2-cell  
169 embryos out of the total number of oocytes inseminated.

170

### 171 **Enhanced IVF**

172 Sperm Energy restriction and Recovery (SER) and Ca<sup>2+</sup> ionophore treatments prior to IVF improve the  
173 rate of fertilization in subfertile and infertile animals (Navarrete et al., 2016; Navarrete et al., 2019).  
174 The following sperm treatments prior to IVF were tested: 1) Control (TYH); 2) Control + Ca<sup>2+</sup>  
175 ionophore; 3) SER; and 4) SER + Ca<sup>2+</sup> ionophore. For each 3-month-old male, one cauda epididymis  
176 was collected and placed in TYH medium (tube A) and the other cauda epididymis was collected and  
177 placed in TYH medium devoid of glucose and pyruvate (SER-TYH, tube B). After 10 minutes of  
178 incubation in 5% CO<sub>2</sub> at 37 °C to allow sperm swim-out, cauda tissues were removed. Sperm  
179 suspensions were centrifuged twice at 150 g for 5 minutes and the sperm pellet was washed with 2 ml  
180 of TYH for tube A and 2 ml of SER-TYH for tube B. After the final wash, sperm pellets were  
181 resuspended in 500 µl of TYH for tube A and 500 µl of SER-TYH for tube B. Each tube was  
182 immediately divided into two 250 µl suspensions and incubated in 5% CO<sub>2</sub> at 37 °C until the sperm  
183 motility from treatments 3 and 4 was significantly slow (about 30 minutes). At that point, Ca<sup>2+</sup>

184 ionophore 4Br-A23187 (Cat. No. C7522, Fisher Scientific) was added to a final concentration of 20  
185  $\mu\text{M}$  for treatment 2 and 5  $\mu\text{M}$  for treatment 4. After 10-minute incubation with  $\text{Ca}^{2+}$  ionophore, 1.5 ml  
186 of TYH was added to all the treatments and immediately centrifuged at 150 g for 5 min. Sperm pellets  
187 were then washed again with TYH and centrifuged at 150 g for 5 minutes. Sperm pellets were  
188 resuspended in 500  $\mu\text{l}$  of TYH and used for insemination of COCs. All the procedures after  
189 insemination were performed as described above for regular IVF.

190

### 191 **Embryo culture**

192 The two-cell embryos from IVF were washed and placed in a dish of equilibrated KSOM media (Cat.  
193 No. MR-106-D, Fisher Scientific) covered by light mineral oil (Cat. No. 0121-1, Fisher Scientific).  
194 Embryo culture dishes were incubated for 3.5 days in 5%  $\text{CO}_2$ , 5%  $\text{O}_2$ , at 37°C. Results are expressed  
195 as percentage of blastocysts out of the 2-cell embryos and percentage of blastocysts out of the total  
196 number of oocytes inseminated.

197

### 198 **Immunofluorescence and super-resolution imaging**

199 After three incisions, cauda epididymides were incubated in PBS at 37°C for 10 min. Swim-out sperm  
200 were placed on slides and fixed in 2% PFA in PBS with 0.2% Triton X-100 overnight. The slides were  
201 incubated with anti-C2CD6 (UP2430, 1:100) or anti-Catsper1 (1:200) antibodies, then with anti-rabbit  
202 FITC-conjugated secondary antibody, and finally mounted with DAPI. Images were captured with an  
203 ORCA digital camera (Hamamatsu Photonics) on a Leica DM5500B microscope. For structured  
204 illumination microscopy (SIM) imaging, images were acquired on a GE DeltaVision OMX SR  
205 imaging system with PCO sCMOS cameras and were processed using softWoRx software.

206

### 207 **Testis microsome extraction**

208 One adult testis (~100 mg) was homogenized on ice in 1ml 0.32 M sucrose solution with 1 $\times$  protease  
209 inhibitor cocktail (Cat No. P8340, Sigma). After centrifugation at 300 g at 4°C for 10 minutes, the  
210 supernatant was transferred to an ultra-centrifuge tube and centrifuged at 100,000 g for one hour. The  
211 pellet containing the microsome fraction was resuspended and solubilized in 5 ml PBS with 1% Triton  
212 X-100 and 1 $\times$  protease inhibitor cocktail by rocking at 4°C for 2 hours. The suspension was  
213 centrifuged at 15,000 g for 30 minutes and the supernatant was collected for Western blot analysis.

214

### 215 **Sperm protein extraction**

216 Sperm ( $\sim 1.3 \times 10^7$ ) were collected from one adult mouse by squeezing the cauda epididymides in PBS  
217 solution and centrifugation at 800 g for 5 minutes at room temperature. Sperm were homogenized in  
218 100  $\mu$ l SDS-EDTA solution (1% SDS, 75 mM NaCl, 24 mM EDTA, pH 6.0) and centrifuged at 5000 g  
219 for 30 minutes at room temperature. 100  $\mu$ l 2 $\times$  SDS-PAGE sample buffer (62.5 mM Tris, pH 6.8, 3%  
220 SDS, 10% glycerol, 5%  $\beta$ -mercaptoethanol, 0.02% bromophenol blue) was added to 100  $\mu$ l of  
221 supernatant. The samples were heated at 95°C for 10 minutes and 20  $\mu$ l of each sample (equivalent to  
222  $1.3 \times 10^6$  sperm) was used for Western blot analysis.

223

## 224 **Cell culture, transfection, and immunoprecipitation**

225 The ORFs of *C2cd6s*, *Efcab9*, *CatSper $\zeta$* , *CatSper2*, *CatSper3*, and *CatSper4* were PCR amplified from  
226 bulk mouse testis cDNAs. The *CatSper1* ORF was amplified from a mouse cDNA clone (Cat. No.  
227 MR224271, Origene). *C2cd6s* was subcloned into pcDNA3.1/myc-His A vector (Cat. No. V800-20,  
228 Invitrogen). The others were TA-cloned to pcDNA3.1/V5-His TOPO TA vectors (Cat. No. K4800-01,  
229 Invitrogen). HEK293T cells were cultured in DMEM medium with 10% FBS in 5% CO<sub>2</sub> at 37°C. 24 to  
230 48 hours after transfection, the cells (3 wells of a 6-well plate) were lysed in 1 ml IP buffer (50 mM  
231 Tris, pH 8.0, 150 mM NaCl, 5 mM MgCl<sub>2</sub>, 1m M DTT, 0.5% deoxycholate, 1% Triton) with 1 $\times$   
232 cocktail of protease inhibitors, incubated at 4°C for one hour, and centrifuged at 12,000 g for 30  
233 minutes. 10  $\mu$ l of supernatant (1%) was set aside as input. The bulk of supernatant ( $\sim 1$  ml) was  
234 incubated with antibodies at 4°C for one hour: 3  $\mu$ l (0.5  $\mu$ g/ $\mu$ l) c-Myc monoclonal antibody (Cat. No.  
235 631206, TaKaRa), or 1  $\mu$ l (1.1  $\mu$ g/ $\mu$ l) anti-V5 antibody (Cat. No. P/N 46-0705, Invitrogen), or 20  $\mu$ l  
236 anti-C2CD6 (UP2429) antibody. 10  $\mu$ l of Dynabeads G or A (Invitrogen) was added for each IP and  
237 incubated at 4°C overnight. Immunoprecipitated proteins were washed five times with the wash buffer  
238 (50 mM Tris, pH 7.5, 250 mM NaCl, 0.1% NP-40, 0.05% deoxycholate) and were eluted in 15  $\mu$ l 2 $\times$   
239 SDS sample buffer at 95°C. Elutes and inputs were separated by SDS-PAGE and transferred to  
240 nitrocellulose membrane. Anti-c-Myc monoclonal, anti-V5, and anti-CatSper1 (gift from Dejian Ren)  
241 (Ren et al., 2001) antibodies were used for Western blotting.

242

## 243 **Results**

### 244 **Identification of a novel evolutionarily conserved sperm flagellar protein**

245 We were interested in interacting proteins of TEX11, a meiosis-specific protein that we previously  
246 identified (Yang et al., 2008; Yang et al., 2015). ALS2CR11 was reported as one of the TEX11-  
247 interacting proteins in the genome-wide protein-protein interaction study (Rual et al., 2005). However,



248 we find that ALS2CR11 (NP\_780409) localizes to sperm flagellum but does not function in meiosis.  
249 Since ALS2CR11 contains a calcium-dependent membrane targeting C2 domain, it has been renamed  
250 as C2CD6 (C2 calcium dependent domain containing 6) (Fig. 1A and 1B) (Nalefski and Falke, 1996).  
251 The *C2cd6* gene is conserved in vertebrates. The transcripts from the *C2cd6* gene locus are very  
252 complex. As we were analyzing the *C2cd6* gene structure on Chromosome 1, we noticed another  
253 uncharacterized gene 3' downstream, which has a large coding exon (~5 kb), and named it *Als2cr11b*  
254 (Fig. 1A). Based on EST (expressed sequence tag) profiling, both *C2cd6* and *Als2cr11b* transcripts are  
255 testis-specific.

256 We generated polyclonal antibodies against a recombinant C2CD6 N-terminal 386-aa protein.  
257 Western blot analysis showed that C2CD6 was present in adult testis but not in ovary or somatic  
258 tissues in mice, demonstrating that C2CD6 is testis-specific (Fig. 1C). Interestingly, C2CD6 appeared  
259 as two major isoforms: C2CD6S (short, ~60 kD) and C2CD6L (long, ~85 kD). To determine the nature  
260 of these two C2CD6 isoforms, we performed RT-PCR, 3'RACE, and sequencing. The presence of two  
261 C2CD6 isoforms was due to alternative splicing (Fig. 1A). The *C2cd6s* transcript (GenBank accession  
262 number: NM\_175200) consists of 13 exons and encodes a protein of 557 aa. The *C2cd6l* transcript  
263 (GenBank accession number: MW717645) is more complex and harbors alternative exon 13,  
264 alternative exon 1 of *Als2cr11b*, and splicing of an intron within *Als2cr11b* exon 5. As a result, the  
265 protein (691 aa) encoded by the *C2cd6l* transcript is larger than C2CD6S (557 aa) but smaller than  
266 ALS2CR11B (1729 aa). C2CD6S and C2CD6L share the first 533 aa and the predicted Ca<sup>2+</sup>-binding  
267 membrane targeting domain (Fig. 1B). Therefore, our C2CD6 antibody recognizes both isoforms. We  
268 then generated polyclonal antibodies against the C-terminal 200 aa of ALS2CR11B. Western blot  
269 analysis identified a protein band of ~180 kD in testis but also in lung and brain at a low abundance,  
270 suggesting that *Als2cr11b* encodes a bona fide protein (Fig. 1C). Neither C2CD6 nor ALS2CR11B  
271 contain predicted transmembrane domains.

272 We immunostained sperm with anti-C2CD6 antibodies. Immunofluorescence analysis revealed  
273 that C2CD6 localized specifically to the principal piece of sperm flagellum (Fig. 1D), showing that  
274 C2CD6 is a novel component of sperm flagella. The C2CD6 signal is strong at the beginning of the  
275 principal piece (at the annulus region) and tapers off toward the end piece. The C2CD6 signal is  
276 specific, since it is absent in *C2cd6*-deficient sperm (Fig. 1D). Noticeably, two distinctive columns of  
277 C2CD6 can be appreciated in the principal piece by widefield fluorescence microscopy (Fig. 1D).  
278 These results demonstrate that C2CD6 is a new component of the sperm flagella.

279

280 **C2CD6 is essential for male fertility and in vivo fertilization**

281 To study the functional requirement of *C2cd6*, we inactivated *C2cd6* by deleting a 1.6-Kb genomic  
282 region, including exon 1 (containing the initiating codon), through gene targeting in ES cells (Fig. 2A).  
283 Homozygous *C2cd6*<sup>-/-</sup> mice were viable and grossly normal. While *C2cd6*<sup>-/-</sup> females had normal  
284 fertility, *C2cd6*<sup>-/-</sup> males were sterile. *C2cd6*<sup>-/-</sup> males produced copulatory plugs, indicating normal  
285 mating behavior. Western blotting analysis showed that both C2CD6S and C2CD6L were absent in  
286 *C2cd6*<sup>-/-</sup> testes, suggesting that the mutant is null (Fig. 2B). Testis weight and sperm count were  
287 comparable between *C2cd6*<sup>+/-</sup> and *C2cd6*<sup>-/-</sup> males (Fig. 2C and 2D). *C2cd6*-deficient sperm displayed  
288 normal morphology. Histology of *C2cd6*<sup>-/-</sup> testes showed apparently normal spermatogenesis (data not  
289 shown) and thus C2CD6, unlike TEX11 (Yang et al., 2008), was not essential for meiosis.

290 *C2cd6*-deficient sperm were apparently motile, however, *C2cd6*<sup>-/-</sup> males were sterile. To probe  
291 the cause of male infertility, we performed in vivo fertilization test. Wild type C57BL/6 females were  
292 injected with PMSG followed by hCG injection, mated with either *C2cd6*<sup>+/-</sup> or *C2cd6*<sup>-/-</sup> males (3 males  
293 per genotype), and copulatory plugs were checked. 24 hours after plug check, eggs/embryos were  
294 flushed from oviducts of plugged females. The number of two-cell embryos and one-cell embryos/eggs  
295 was counted. The majority of embryos (40/59 = 68%) from females plugged by *C2cd6*<sup>+/-</sup> males were at  
296 the 2-cell stage, in contrast, only unfertilized eggs (a total of 51) were obtained from females plugged  
297 by *C2cd6*<sup>-/-</sup> males (Fig. 2E). These data demonstrate that C2CD6 is required for fertilization *in vivo*.

298 To determine the capability of *C2cd6*-deficient sperm in egg activation and embryo  
299 development, we performed ICSI (intracytoplasmic sperm injection). Out of 50 oocytes injected with  
300 *C2cd6*-deficient sperm, 34 embryos reached the 2-cell stage and 20 of them further developed to the  
301 blastocyst stage. This result shows that *C2cd6*-deficient sperm can fertilize oocytes by ICSI and  
302 support embryo development.

### 303 304 **C2CD6 is required for in vitro fertilization and hyperactive motility**

305 We next asked whether *C2cd6*-deficient sperm can fertilize oocytes in vitro. We performed in vitro  
306 fertilization (IVF) assays using cumulus-oocyte complexes from wild type CD1 females (Table 1). An  
307 average fertilization rate of 59 % vs 2 % was obtained when oocytes were incubated with *C2cd6*<sup>+/-</sup> vs  
308 *C2cd6*-deficient sperm (Fig. 3A). Only embryos derived from *C2cd6*<sup>+/-</sup> sperm developed to blastocysts  
309 (76%) after culture in KSOM media (Fig. 3B). The observed 2% fertilization rate obtained with *C2cd6*<sup>-/-</sup>  
310 sperm was likely due to the low frequency of spontaneous parthenogenetic activation of oocytes (Xu  
311 et al., 1997). Therefore, these data indicate that C2CD6 is essential for fertilization in vitro.

312 To determine if the in vitro fertilization failure is related to sperm motility, we performed  
313 CASA (computer assisted sperm analysis) immediately after sperm swim-out from epididymis (T0)

314 and after 60 minutes of incubation under capacitating conditions (T60). No differences in total or  
315 progressive sperm motility were found between *C2cd6<sup>+/-</sup>* and *C2cd6<sup>-/-</sup>* males (Fig. 3C and 3D).  
316 Nevertheless, *C2cd6*-deficient sperm failed to acquire hyperactivated motility after 60 minutes of  
317 incubation under capacitating conditions (Fig. 3E). This could be the cause of the infertility phenotype  
318 in *C2cd6<sup>-/-</sup>* males, since acquisition of hyperactivated motility is essential for fertilization.

319 We next evaluated the possibility of restoring fertility of the *C2cd6*-deficient sperm in vitro.  
320 We applied two sperm treatments prior to IVF that have been proven to restore fertility of other  
321 infertile and subfertile mouse models (Navarrete, Felipe A. et al., 2016; Navarrete, Felipe A. et al.,  
322 2019). Transient incubations with Ca<sup>2+</sup> ionophore (ionophore) and sperm energy restriction (SER)  
323 produced a moderate increase in the fertilization rates of *C2cd6*-deficient sperm: 6.3% and 18.8%  
324 respectively (Table 2). Strikingly, the combination of SER and ionophore treatments of *C2cd6*-  
325 deficient sperm induced an average fertilization rate of 58.8% as a total of 50 2-cell embryos out of 85  
326 inseminated oocytes were obtained (Table 2). To analyze embryo development in vitro, the obtained 2-  
327 cell embryos were further cultured in KSOM media. We observed a blastocyst development rate of  
328 22% in the ionophore treatment-derived embryos, 100% in the SER-derived embryos, and 63% in the  
329 SER + ionophore-derived embryos. Although each sperm treatment was able to overcome the  
330 infertility phenotype of *C2cd6<sup>-/-</sup>* males in vitro, the combination of SER and ionophore treatments was  
331 the most effective.

332

### 333 **C2CD6-dependent CatSper assembly in sperm flagella**

334 CatSper, the flagellar Ca<sup>2+</sup> ion channel, localizes to the principal piece (Fig. 4A) (Chung et al.,  
335 2017; Ren et al., 2001). C2CD6 localization to the sperm flagella (Fig. 1D) is strikingly similar to  
336 CatSper localization. Moreover, using comparative proteomics, C2CD6 was shown to be one of the  
337 proteins displaying reduced abundance in CatSper1-deficient sperm (Hwang et al., 2019). Therefore,  
338 we examined CatSper1 localization in the absence of C2CD6 by immunofluorescence. The CatSper1  
339 signal was severely reduced in *C2cd6<sup>-/-</sup>* sperm (Fig. 4A). We also performed super-resolution imaging  
340 analysis of CatSper1 and C2CD6 localization in sperm flagellum. As previously reported, CatSper1  
341 formed quadrilateral columns in wild type flagellum (Fig. 4B). C2CD6 also appeared in columns but  
342 was less organized than CatSper1 columns in wild type (Fig. 4B). In *C2cd6<sup>-/-</sup>* sperm, CatSper1 signals  
343 were sharply reduced, disorganized, discontinuous, and preferentially distributed to the distal end of  
344 the principal piece (Fig. 4B).

345 CatSper complex is partitioned into microsomes (vesicle-like structures formed from pieces of  
346 endoplasmic reticulum) in testis extracts (Chung et al., 2017). We prepared microsomes from wild type

347 and *C2cd6*<sup>-/-</sup> testes (Fig. 4C). C2CD6, like CatSper1, was present in testicular microsome fractions. In  
348 addition, CatSper1 was abundant in microsome fractions from *C2cd6*<sup>-/-</sup> testes (Fig. 4C), suggesting that  
349 synthesis of CatSper is not affected in *C2cd6*<sup>-/-</sup> testes. We next performed Western blotting analysis of  
350 sperm extracts. As expected, both C2CD6 and CatSper1 were present in wild type and *C2cd6*<sup>+/-</sup> sperm  
351 extracts (Fig. 4D). However, CatSper1 abundance was dramatically reduced in *C2cd6*<sup>-/-</sup> sperm extract  
352 (Fig. 4D). Taken together, our results demonstrate that the CatSper ion channel complex is abundant in  
353 the testis but fail to incorporate into sperm flagella in the absence of C2CD6. Therefore, C2CD6 is  
354 required for assembly of the CatSper channel complex in sperm flagella.

355 We next sought to address whether CatSper is required for C2CD6 localization. Both CatSper1  
356 and C2CD6 were detected in *CatSper1*<sup>+/-</sup> testis microsome extract (Fig. 4E). C2CD6 was present in  
357 *CatSper1*<sup>-/-</sup> testis microsome extract and its abundance was comparable with that in *CatSper1*<sup>+/-</sup> testis  
358 (Fig. 4E). As expected, CatSper1 was absent in *CatSper1*<sup>-/-</sup> flagellum (Fig. 4F). C2CD6 was sharply  
359 reduced in *CatSper1*<sup>-/-</sup> flagellum (Fig. 4G). This result is consistent with the reduced abundance of  
360 C2CD6 (formerly known as ALS2CR11) in *CatSper1*<sup>-/-</sup> sperm shown by quantitative proteomic  
361 analysis (Hwang et al., 2019). These results demonstrate that CatSper is critical for C2CD6  
362 localization in sperm flagella. Therefore, the inter-dependent localization of C2CD6 and CatSper1  
363 suggests that C2CD6 might be an essential component of the CatSper complex.

364

### 365 **C2CD6 interacts with components of the CatSper complex**

366 To investigate the connection of C2CD6 with the CatSper channel complex, we co-expressed C2CD6  
367 with CatSper complex components in HEK293T cells and tested their interaction by co-  
368 immunoprecipitation. C2CD6 and all CatSper components are only expressed in testis and remain in  
369 sperm but are absent in somatic cells such as 293T cells. The abundance of C2CD6 in transfected  
370 HEK293T cells was low but can be dramatically enriched by immunoprecipitation (Fig. 5). The full-  
371 length C2CD6 migrated at 75 kDa and a slightly smaller isoform was also present in the  
372 immunoprecipitated fraction (Fig. 5A). CatSper1 was present in the C2CD6 complex (Fig. 5A).  
373 CatSper2 was also in complex with C2CD6 but the association was weak (Fig. 5B). CatSper3 was  
374 strongly associated with C2CD6 (Fig. 5C). CatSper4 was readily detected in C2CD6-  
375 immunoprecipitated proteins, indicating strong interaction between CatSper4 and C2CD6 (Fig. 5D).  
376 EFCAB9 was abundant in C2CD6-immunoprecipitated proteins, showing that EFCAB9 is strongly  
377 associated with C2CD6 (Fig. 5E). However, we did not detect interaction between C2CD6 and  
378 CatSperz (TEX40) (Fig. 5F). Collectively, C2CD6 interacts with the core components of the CatSper  
379 complex (Fig. 5G).

380

## 381 **Discussion**

382 Here we demonstrate that C2CD6 is a novel and essential subunit of the CatSper complex, in addition  
383 to the ten known subunits (Fig. 5G). Four core  $\alpha$  subunits, CatSper1-4, form the membrane-spanning  
384  $\text{Ca}^{2+}$ -selective pore. C2CD6 interacts with all four  $\alpha$  subunits suggesting that it directly binds to the  
385 CatSper channel core. In addition, C2CD6 interacts with EFCAB9 but not with CatSperZ, a partner of  
386 EFCAB9. We postulate that C2CD6 plays several possible roles in the CatSper channel function. First,  
387 C2CD6 might be a critical structural subunit of CatSper. The decrease of CatSper1 in the C2CD6-  
388 deficient sperm and the decrease of C2CD6 protein in CatSper1-deficient sperm suggest that without  
389 C2CD6, the CatSper complex is not fully assembled. CatSper subunits localize in linear quadrilateral  
390 domains along the sperm principal piece, and the localization of CatSper1 is disrupted in animals  
391 lacking other subunits such as EFCAB9, CatSper $\zeta$ , and CatSper $\epsilon$  (Chung et al., 2011; Chung et al.,  
392 2014; Chung et al., 2017). Consistent with C2CD6 as a novel subunit of the CatSper channel complex,  
393 we find that CatSper1 is drastically reduced in *C2cd6*-deficient sperm and displays disrupted  
394 quadrilateral domain localization in the principal piece. Second, C2CD6 contains a calcium-dependent  
395 membrane-targeting C2 domain. This domain is found in signaling proteins that interact with the  
396 cellular membrane (Nalefski and Falke, 1996). This raises the possibility that C2CD6 might facilitate  
397 targeting of assembled CatSper complexes to the sperm flagellar plasma membrane or insertion into  
398 the membrane. Indeed, CatSper1 is present in testis but not in sperm from *C2cd6*<sup>-/-</sup> males, indicating  
399 that the CatSper complex is unstable without C2CD6. Similar results were found when each of the  
400 other CatSper subunits was individually removed. In each of these cases, the remaining subunits are  
401 expressed in the testes but are absent in mature sperm (Qi et al., 2007). Third, C2CD6 might function  
402 as a  $\text{Ca}^{2+}$  sensor for CatSper independently or as a complex with EFCAB9. Notably, the CatSper  
403 channel is compromised but still conducts currents in EFCAB9-deficient sperm (Hwang et al., 2019).  
404 In EFCAB9-deficient sperm, C2CD6 might be responsible for  $\text{Ca}^{2+}$  sensing.

405 C2CD6 exists as at least two isoforms. Both isoforms contain the C2 domain and are present in  
406 sperm. It is not known whether these two isoforms are functionally redundant or have isoform-specific  
407 functions. Intriguingly, CatSper $\delta$  also has two isoforms resulting from alternative splicing (Chung et  
408 al., 2011). In addition, C2CD6 (previously known as ALS2CR11) is tyrosine phosphorylated upon  
409 capacitation (Chung et al., 2014). The physiological consequence of this phosphorylation on C2CD6 is  
410 unknown. The *Als2cr11b* gene encodes a bona fide protein in testis (Fig. 1C). Like *C2cd6*, *Als2cr11b*  
411 is conserved in vertebrates. Future study is necessary to investigate whether ALS2CR11B is a subunit

412 of the CatSper complex. Genetic ablation of *Als2cr11b* alone without disruption of *C2cd6* is  
413 challenging, because *Als2cr11b* shares exons with *C2cd6l* (Fig. 1A).

414 *C2cd6*<sup>-/-</sup> sperm do not fertilize oocytes in vivo or in vitro. The sterility phenotype is caused by  
415 the failure in induction of hyperactivated motility during sperm capacitation. Hyperactivated motility is  
416 characterized by a high-amplitude asymmetrical beating of the sperm flagellum (Suarez and Osman,  
417 1987). This flagellar beating pattern is mainly regulated by sperm intracellular Ca<sup>2+</sup> concentrations  
418 ([Ca<sup>2+</sup>]<sub>i</sub>), which are maintained by ion channels and pumps in the plasma membrane (Visconti, Pablo  
419 E. et al., 2011). Two of the most important sperm [Ca<sup>2+</sup>]<sub>i</sub> regulators are the CatSper channel that is  
420 essential for the entrance of Ca<sup>2+</sup> to the sperm (Ren et al., 2001), and the Ca<sup>2+</sup> efflux pump PMCA4  
421 that is required for Ca<sup>2+</sup> clearance (Wennemuth et al., 2003). The proper assembly and function of the  
422 CatSper channel are essential for acquisition of sperm hyperactivated motility and fertility (Chung et  
423 al., 2011; Chung et al., 2017; Hwang et al., 2019; Ren et al., 2001). Consistent with our conclusion that  
424 C2CD6 is a novel subunit of the CatSper channel complex, *C2cd6*-deficient sperm fail to achieve  
425 hyperactivated motility after incubation under capacitating conditions.

426 Ca<sup>2+</sup> is a second messenger with pivotal roles in activating (or inhibiting) downstream effectors  
427 during sperm capacitation (Navarrete, F. A. et al., 2015). The transient treatment of sperm with Ca<sup>2+</sup>  
428 ionophore A23187 can bypass the activation of the main molecular pathway critical for acquisition of  
429 fertilizing capacity during sperm capacitation: the cAMP/PKA pathway (Tateno et al., 2013). This  
430 transient sperm ionophore treatment was applied prior to IVF and successfully reversed the male  
431 sterility phenotype of *CatSper1*<sup>-/-</sup>, *sAC*<sup>-/-</sup>, and *Slo3*<sup>-/-</sup> mice as moderate fertilization was achieved  
432 (Navarrete et al., 2016). In line with these previous observations, the ionophore treatment prior to IVF  
433 in *C2cd6*-deficient sperm reversed the sterility phenotype, indicating that an increase of intracellular  
434 Ca<sup>2+</sup> is sufficient to restore fertility in this mouse model. We have recently developed another sperm  
435 treatment that improves fertilization rates and embryo development of sub-fertile mouse models by  
436 manipulation of the sperm metabolism (Navarrete et al., 2019). When applied prior to IVF in  
437 *CatSper1*<sup>-/-</sup> sperm, this Sperm Energy restriction and Recovery (SER) treatment was not able to restore  
438 fertility; however, a combination of the ionophore A23187 and the SER treatments induced a  
439 synergistic effect on fertilization rates and embryo development in the *CatSper1*<sup>-/-</sup> model (Navarrete et  
440 al., 2019). The same synergistic effect was observed on *C2cd6*-deficient sperm. Interestingly, while the  
441 SER treatment did not rescue the sterility phenotype of *CatSper1*<sup>-/-</sup> mice (Navarrete et al 2019), the  
442 application of SER treatment alone was able to overcome the sterility phenotype of the *C2cd6*<sup>-/-</sup> mice.  
443 This could be related to our recent findings that SER treatment induces an elevation of [Ca<sup>2+</sup>]<sub>i</sub> in  
444 mouse sperm from wild type and *Catsper1*<sup>-/-</sup> animals (Sánchez-Cárdenas et al., 2021).

445           The CatSper channel is essential for sperm hyperactivation and male fertility in both mice and  
446 humans. The CatSper subunits are only expressed in testis and sperm. Traditionally, ion channels are  
447 druggable targets. For these reasons, the CatSper channel has been proposed as a target for male  
448 contraception with minimal side effects. However, reconstitution of CatSper in a heterologous system  
449 has not been achieved, despite that CatSper was discovered two decades ago (Ren et al., 2001). The  
450 lack of a heterologous system impedes drug discovery efforts for small molecule inhibitors of CatSper.  
451 The challenges for developing a CatSper heterologous system are several fold. First, the CatSper ion  
452 channel is extremely complex. It is still possible that not all CatSper-associated proteins are known.  
453 C2CD6 is the newest CatSper subunit. Second, the CatSper assembly might require chaperones. The  
454 CatSper complex is associated with a testis-specific chaperone – HSPA2 (Chung et al., 2011;Zhu et al.,  
455 1997). Third, sperm flagellum is a unique ciliary structure. CatSper forms organized linear domains  
456 along the principal piece. Organization of these nanodomains might depend on other flagellar unique  
457 structures such as fibrous sheath, which are absent in heterologous cells. The identification of C2CD6  
458 might facilitate successful development of a heterologous CatSper system, which is not only critical  
459 for drug development but also provide an amenable system to dissect the mechanistic role of each  
460 subunit in CatSper.

461

#### 462 **Acknowledgements**

463 We thank Dejian Ren for anti-CatSper1 antibody. This study was supported by NIH/National Institute  
464 of General Medical Sciences GM118052 (PJW), Eunice Kennedy Shriver National Institute of Child  
465 Health and Human Development HD069592 and HD068157 (PJW), HD38082 and HD088571 (PEV),  
466 and National Research Service Award T32 GM108556 (DAT).

467

#### 468 **Author contributions**

469 F.Y. and P.J.W. conceptualized the study. F.Y. generated and characterized the *C2cd6* knockout mice.  
470 M.G.G., D.A.T., and P.E.V. contributed the CASA, IVF, and in vitro sperm treatment data; N.A.L.  
471 performed blastocyst injection and generated chimeric mice; G.R. contributed to the super resolution  
472 microscopy experiments; P.J.W., F.Y., M.G.G., and P.E.V. wrote the manuscript. All the authors  
473 commented on the manuscript.

474

#### 475 **References**

- 476 **Avenarius, M. R., Hildebrand, M. S., Zhang, Y., Meyer, N. C., Smith, L. L., Kahrizi, K.,**  
477 **Najmabadi, H. and Smith, R. J. (2009).** Human Male Infertility Caused by Mutations in the  
478 CATSPER1 Channel Protein. *Am. J. Hum. Genet.* **84**, 505-510.
- 479 **Brenker, C., Zhou, Y., Muller, A., Echeverry, F. A., Trotschel, C., Poetsch, A., Xia, X. M.,**  
480 **Bonigk, W., Lingle, C. J., Kaupp, U. B. et al. (2014).** The Ca<sup>2+</sup>-Activated K<sup>+</sup> Current of Human  
481 Sperm is Mediated by Slo3. *Elife* **3**, e01438.
- 482 **Brown, S. G., Miller, M. R., Lishko, P. V., Lester, D. H., Publicover, S. J., Barratt, C. L. R. and**  
483 **Martins Da Silva, S. (2018).** Homozygous in-Frame Deletion in CATSPERE in a Man Producing  
484 Spermatozoa with Loss of CatSper Function and Compromised Fertilizing Capacity. *Hum. Reprod.* **33**,  
485 1812-1816.
- 486 **Cao, W., Gerton, G. L. and Moss, S. B. (2006).** Proteomic Profiling of Accessory Structures from the  
487 Mouse Sperm Flagellum. *Mol. Cell. Proteomics* **5**, 801-810.
- 488 **Carlson, A. E., Quill, T. A., Westenbroek, R. E., Schuh, S. M., Hille, B. and Babcock, D. F.**  
489 **(2005).** Identical Phenotypes of CatSper1 and CatSper2 Null Sperm. *J. Biol. Chem.* **280**, 32238-32244.
- 490 **Carlson, A. E., Westenbroek, R. E., Quill, T., Ren, D., Clapham, D. E., Hille, B., Garbers, D. L.**  
491 **and Babcock, D. F. (2003).** CatSper1 Required for Evoked Ca<sup>2+</sup> Entry and Control of Flagellar  
492 Function in Sperm. *Proc. Natl. Acad. Sci. U. S. A.* **100**, 14864-14868.
- 493 **Chang, M. C. (1951).** Fertilizing Capacity of Spermatozoa Deposited into the Fallopian Tubes. *Nature*  
494 **168**, 697-698.



- 495 **Chavez, J. C., Ferreira, J. J., Butler, A., De La Vega Beltran, J. L., Trevino, C. L., Darszon, A.,**  
496 **Salkoff, L. and Santi, C. M.** (2014). SLO3 K<sup>+</sup> Channels Control Calcium Entry through CATSPER  
497 Channels in Sperm. *J. Biol. Chem.* **289**, 32266-32275.
- 498 **Chung, J. J., Miki, K., Kim, D., Shim, S. H., Shi, H. F., Hwang, J. Y., Cai, X., Iseri, Y., Zhuang,**  
499 **X. and Clapham, D. E.** (2017). CatSperzeta Regulates the Structural Continuity of Sperm Ca<sup>2+</sup>  
500 Signaling Domains and is Required for Normal Fertility. *Elife* **6**, 10.7554/eLife.23082.
- 501 **Chung, J. J., Navarro, B., Krapivinsky, G., Krapivinsky, L. and Clapham, D. E.** (2011). A Novel  
502 Gene Required for Male Fertility and Functional CATSPER Channel Formation in Spermatozoa. *Nat.*  
503 *Commun.* **2**, 153.
- 504 **Chung, J. J., Shim, S. H., Everley, R. A., Gygi, S. P., Zhuang, X. and Clapham, D. E.** (2014).  
505 Structurally Distinct Ca<sup>2+</sup> Signaling Domains of Sperm Flagella Orchestrate Tyrosine  
506 Phosphorylation and Motility. *Cell* **157**, 808-822.
- 507 **Geng, Y., Ferreira, J. J., Dzikunu, V., Butler, A., Lybaert, P., Yuan, P., Magleby, K. L., Salkoff,**  
508 **L. and Santi, C. M.** (2017). A Genetic Variant of the Sperm-Specific SLO3 K<sup>(+)</sup> Channel has Altered  
509 pH and Ca<sup>2+</sup> Sensitivities. *J. Biol. Chem.* **292**, 8978-8987.
- 510 **Harlow, E. and Lane, D.** (1998). *Using Antibodies: A Laboratory Manual*. Cold Spring Harbor: Cold  
511 Spring Harbor Laboratory Press.
- 512 **Hwang, J. Y., Mannowetz, N., Zhang, Y., Everley, R. A., Gygi, S. P., Bewersdorf, J., Lishko, P.**  
513 **V. and Chung, J. J.** (2019). Dual Sensing of Physiologic pH and Calcium by EFCAB9 Regulates  
514 Sperm Motility. *Cell* **177**, 1480-1494.e19.

- 515 **Jin, J., Jin, N., Zheng, H., Ro, S., Tafolla, D., Sanders, K. M. and Yan, W.** (2007). Catsper3 and  
516 Catsper4 are Essential for Sperm Hyperactivated Motility and Male Fertility in the Mouse. *Biol.*  
517 *Reprod.* **77**, 37-44.
- 518 **Kirichok, Y., Navarro, B. and Clapham, D. E.** (2006). Whole-Cell Patch-Clamp Measurements of  
519 Spermatozoa Reveal an Alkaline-Activated Ca<sup>2+</sup> Channel. *Nature* **439**, 737-740.
- 520 **Lin, S., Ke, M., Zhang, Y., Yan, Z. and Wu, J.** (2021). Structure of a Mammalian Sperm Cation  
521 Channel Complex. *Nature*.
- 522 **Lishko, P. V., Botchkina, I. L., Fedorenko, A. and Kirichok, Y.** (2010). Acid Extrusion from  
523 Human Spermatozoa is Mediated by Flagellar Voltage-Gated Proton Channel. *Cell* **140**, 327-337.
- 524 **Lishko, P. V., Botchkina, I. L. and Kirichok, Y.** (2011). Progesterone Activates the Principal Ca<sup>2+</sup>  
525 Channel of Human Sperm. *Nature* **471**, 387-391.
- 526 **Liu, J., Xia, J., Cho, K. H., Clapham, D. E. and Ren, D.** (2007). CatSperbeta, a Novel  
527 Transmembrane Protein in the CatSper Channel Complex. *J. Biol. Chem.* **282**, 18945-18952.
- 528 **Luo, T., Chen, H. Y., Zou, Q. X., Wang, T., Cheng, Y. M., Wang, H. F., Wang, F., Jin, Z. L.,**  
529 **Chen, Y., Weng, S. Q. et al.** (2019). A Novel Copy Number Variation in CATSPER2 Causes  
530 Idiopathic Male Infertility with Normal Semen Parameters. *Hum. Reprod.* **34**, 414-423.
- 531 **Miki, K. and Clapham, D. E.** (2013). Rheotaxis Guides Mammalian Sperm. *Curr. Biol.* **23**, 443-452.
- 532 **Miller, M. R., Mannowetz, N., Iavarone, A. T., Safavi, R., Gracheva, E. O., Smith, J. F., Hill, R.**  
533 **Z., Bautista, D. M., Kirichok, Y. and Lishko, P. V.** (2016). Unconventional Endocannabinoid  
534 Signaling Governs Sperm Activation Via the Sex Hormone Progesterone. *Science* **352**, 555-559.

- 535 **Nalefski, E. A. and Falke, J. J.** (1996). The C2 Domain Calcium-Binding Motif: Structural and  
536 Functional Diversity. *Protein Sci.* **5**, 2375-2390.
- 537 **Navarrete, F. A., Garcia-Vazquez, F. A., Alvau, A., Escoffier, J., Krapf, D., Sanchez-Cardenas,**  
538 **C., Salicioni, A. M., Darszon, A. and Visconti, P. E.** (2015). Biphasic Role of Calcium in Mouse  
539 Sperm Capacitation Signaling Pathways. *J. Cell. Physiol.* **230**, 1758-1769.
- 540 **Navarrete, F. A., Aguila, L., Martin-Hidalgo, D., Tourzani, D. A., Luque, G. M., Ardestani, G.,**  
541 **Garcia-Vazquez, F. A., Levin, L. R., Buck, J., Darszon, A. et al.** (2019). Transient Sperm Starvation  
542 Improves the Outcome of Assisted Reproductive Technologies. *Frontiers in cell and developmental*  
543 *biology* **7**, 262.
- 544 **Navarrete, F. A., Alvau, A., Lee, H. C., Levin, L. R., Buck, J., Leon, P. M., Santi, C. M., Krapf,**  
545 **D., Mager, J., Fissore, R. A. et al.** (2016). Transient Exposure to Calcium Ionophore Enables in Vitro  
546 Fertilization in Sterile Mouse Models. *Scientific reports* **6**, 33589.
- 547 **Qi, H., Moran, M. M., Navarro, B., Chong, J. A., Krapivinsky, G., Krapivinsky, L., Kirichok, Y.,**  
548 **Ramsey, I. S., Quill, T. A. and Clapham, D. E.** (2007). All Four CatSper Ion Channel Proteins are  
549 Required for Male Fertility and Sperm Cell Hyperactivated Motility. *Proc. Natl. Acad. Sci. U. S. A.*  
550 **104**, 1219-1223.
- 551 **Quill, T. A., Sugden, S. A., Rossi, K. L., Doolittle, L. K., Hammer, R. E. and Garbers, D. L.**  
552 (2003). Hyperactivated Sperm Motility Driven by CatSper2 is Required for Fertilization. *Proc. Natl.*  
553 *Acad. Sci. U. S. A.* **100**, 14869-14874.
- 554 **Ren, D., Navarro, B., Perez, G., Jackson, A. C., Hsu, S., Shi, Q., Tilly, J. L. and Clapham, D. E.**  
555 (2001). A Sperm Ion Channel Required for Sperm Motility and Male Fertility. *Nature* **413**, 603-609.

- 556 **Rual, J. F., Venkatesan, K., Hao, T., Hirozane-Kishikawa, T., Dricot, A., Li, N., Berriz, G. F.,**  
557 **Gibbons, F. D., Dreze, M., Ayivi-Guedehoussou, N. et al. (2005).** Towards a Proteome-Scale Map of  
558 the Human Protein-Protein Interaction Network. *Nature* **437**, 1173-1178.
- 559 **Sánchez-Cárdenas, C., Romarowski, A., Orta, G., De la Vega-Beltrán, José Luis, Martín-**  
560 **Hidalgo, D., Hernández-Cruz, A., Visconti, P. E. and Darszon, A. (2021).** Starvation Induces an  
561 Increase in Intracellular Calcium and Potentiates the Progesterone-induced Mouse Sperm Acrosome  
562 Reaction. *The FASEB journal* **35**, e21528-n/a.
- 563 **Santi, C. M., Martínez-Lopez, P., de la Vega-Beltran, J. L., Butler, A., Alisio, A., Darszon, A. and**  
564 **Salkoff, L. (2010).** The SLO3 Sperm-Specific Potassium Channel Plays a Vital Role in Male Fertility.  
565 *FEBS Lett.* **584**, 1041-1046.
- 566 **Schreiber, M., Wei, A., Yuan, A., Gaut, J., Saito, M. and Salkoff, L. (1998).** Slo3, a Novel pH-  
567 Sensitive K<sup>+</sup> Channel from Mammalian Spermatocytes. *J. Biol. Chem.* **273**, 3509-3516.
- 568 **Smith, J. F., Syritsyna, O., Fellous, M., Serres, C., Mannowetz, N., Kirichok, Y. and Lishko, P. V.**  
569 (2013). Disruption of the Principal, Progesterone-Activated Sperm Ca<sup>2+</sup> Channel in a CatSper2-  
570 Deficient Infertile Patient. *Proc. Natl. Acad. Sci. U. S. A.* **110**, 6823-6828.
- 571 **Stauss, C. R., Votta, T. J. and Suarez, S. S. (1995).** Sperm Motility Hyperactivation Facilitates  
572 Penetration of the Hamster Zona Pellucida. *Biol. Reprod.* **53**, 1280-1285.
- 573 **Strunker, T., Goodwin, N., Brenker, C., Kashikar, N. D., Weyand, I., Seifert, R. and Kaupp, U.**  
574 **B. (2011).** The CatSper Channel Mediates Progesterone-Induced Ca<sup>2+</sup> Influx in Human Sperm. *Nature*  
575 **471**, 382-386.

- 576 **Suarez, S. S. and Osman, R. A.** (1987). Initiation of Hyperactivated Flagellar Bending in Mouse  
577 Sperm within the Female Reproductive Tract. *Biol. Reprod.* **36**, 1191-1198.
- 578 **Suarez, S. S.** (2016). Mammalian Sperm Interactions with the Female Reproductive Tract. *Cell Tissue*  
579 *Res.* **363**, 185-194.
- 580 **Tateno, H., Krapf, D., Hino, T., Sanchez-Cardenas, C., Darszon, A., Yanagimachi, R. and**  
581 **Visconti, P. E.** (2013). Ca<sup>2+</sup> Ionophore A23187 can make Mouse Spermatozoa Capable of Fertilizing  
582 in Vitro without Activation of cAMP-Dependent Phosphorylation Pathways. *Proc. Natl. Acad. Sci. U.*  
583 *S. A.* **110**, 18543-18548.
- 584 **Visconti, P. E., Bailey, J. L., Moore, G. D., Pan, D., Olds-Clarke, P. and Kopf, G. S.** (1995).  
585 Capacitation of Mouse Spermatozoa. I. Correlation between the Capacitation State and Protein  
586 Tyrosine Phosphorylation. *Development* **121**, 1129-1137.
- 587 **Visconti, P. E., Krapf, D., de la Vega-Beltrán, José Luis, Acevedo, J. J. and Darszon, A.** (2011).  
588 Ion Channels, Phosphorylation and Mammalian Sperm Capacitation. *Asian journal of andrology* **13**,  
589 395-405.
- 590 **Vishwakarma, P.** (1962). The pH and Bicarbonate-Ion Content of the Oviduct and Uterine Fluids.  
591 *Fertil. Steril.* **13**, 481-485.
- 592 **Vyklicka, L. and Lishko, P. V.** (2020). Dissecting the Signaling Pathways Involved in the Function of  
593 Sperm Flagellum. *Curr. Opin. Cell Biol.* **63**, 154-161.
- 594 **Wang, H., Liu, J., Cho, K. H. and Ren, D.** (2009). A Novel, Single, Transmembrane Protein  
595 CATSPERG is Associated with CATSPER1 Channel Protein. *Biol. Reprod.* **81**, 539-544.

- 596 **Wang, H., McGoldrick, L. L. and Chung, J. J.** (2021). Sperm Ion Channels and Transporters in  
597 Male Fertility and Infertility. *Nat. Rev. Urol.* **18**, 46-66.
- 598 **Wennemuth, G., Babcock, D. F. and Hille, B.** (2003). Calcium Clearance Mechanisms of Mouse  
599 Sperm. *J. Gen. Physiol.* **122**, 115-128.
- 600 **Xu, Z., Abbott, A., Kopf, G. S., Schultz, R. M. and Ducibella, T.** (1997). Spontaneous Activation of  
601 Ovulated Mouse Eggs: Time-Dependent Effects on M-Phase Exit, Cortical Granule Exocytosis,  
602 Maternal Messenger Ribonucleic Acid Recruitment, and Inositol 1,4,5-Trisphosphate Sensitivity. *Biol.*  
603 *Reprod.* **57**, 743-750.
- 604 **Yang, F., Gell, K., van der Heijden, G. W., Eckardt, S., Leu, N. A., Page, D. C., Benavente, R.,**  
605 **Her, C., Hoog, C., McLaughlin, K. J. et al.** (2008). Meiotic Failure in Male Mice Lacking an X-  
606 Linked Factor. *Genes Dev.* **22**, 682-691.
- 607 **Yang, F., Silber, S., Leu, N. A., Oates, R. D., Marszalek, J. D., Skaletsky, H., Brown, L. G.,**  
608 **Rozen, S., Page, D. C. and Wang, P. J.** (2015). TEX11 is Mutated in Infertile Men with Azoospermia  
609 and Regulates Genome-Wide Recombination Rates in Mouse. *EMBO Mol. Med.* **7**, 1198-1210.
- 610 **Zeng, X. H., Yang, C., Kim, S. T., Lingle, C. J. and Xia, X. M.** (2011). Deletion of the Slo3 Gene  
611 Abolishes Alkalization-Activated K<sup>+</sup> Current in Mouse Spermatozoa. *Proc. Natl. Acad. Sci. U. S. A.*  
612 **108**, 5879-5884.
- 613 **Zhu, D., Dix, D. J. and Eddy, E. M.** (1997). HSP70-2 is Required for CDC2 Kinase Activity in  
614 Meiosis I of Mouse Spermatocytes. *Development* **124**, 3007-3014.
- 615  
616  
617

618

619 **Table 1.** In vitro fertilization

Genotype	Total oocytes	Unfertilized	Degraded	2-cell embryos	Blastocysts
<i>C2cd6</i> <sup>+/-</sup> (n = 3)	202	95	13	94	74
<i>C2cd6</i> <sup>-/-</sup> (n = 3)	186	168	14	4	0

620

621

622

623

624

625

626

627

628

629

630

631

632

633

634

635

636

637

638

639

640

641

642

643

644

645

646

647

648 **Table 2.** Ionophore and SER treatments

	Genotype	Control	Control + Ionophore	SER	SER + Ionophore
Fertilization (%)	<i>C2cd6<sup>+/-</sup></i>	222/405 (54.8)	46/48 (95.8)	-	-
	<i>C2cd6<sup>-/-</sup></i>	10/389 (2.6)	6/96 (6.3)	15/80 (18.8)	50/85 (58.8)
Blastocyst/2-cell (%)	<i>C2cd6<sup>+/-</sup></i>	144/222 (64.9)	43/46 (93.5)	-	-
	<i>C2cd6<sup>-/-</sup></i>	0/10 (0)	2/5 (22.2)	14/14 (100)	31/50 (62.7)

649

650

651

652



## Figures

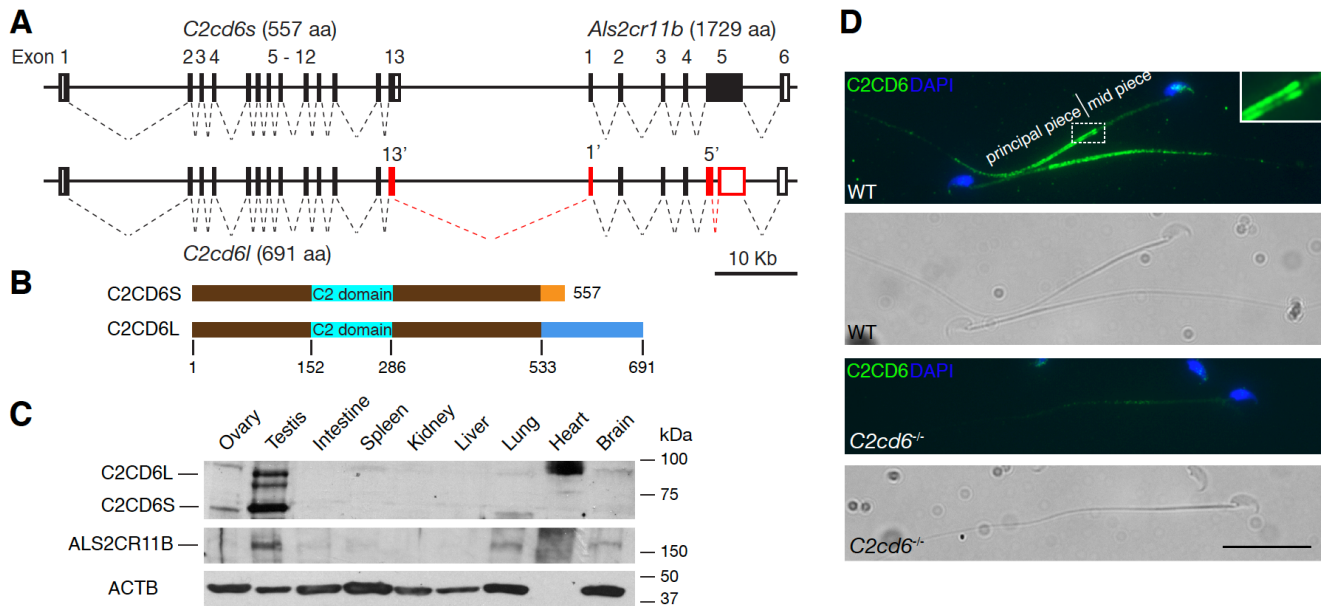


**Figure 1. C2CD6 localizes to the principal piece of sperm flagella.** (A) Gene structures of *C2cd6* and *Als2cr11b* on Chromosome 1. Coding regions of exons are shown in black boxes. 5' and 3' untranslated regions (UTR) are shown as open boxes. Alternative exons of *C2cd6l* are shown in red. Alternative exons 13' and 1' are in frame. Splicing of an intron within *Als2cr11b* exon 5 resulting in early frame shift in the *C2cd6l* transcript. GenBank accession numbers for cDNA sequences: *C2cd6l*, MW717645; *C2cd6s*, NM\_175200; *Als2cr11b*, XM\_011238634. (B) Schematic diagram of two C2CD6 protein isoforms. The N-terminal 533 residues are identical. The Ca<sup>2+</sup> binding membrane targeting C2 domain is predicted based on Phyre2. (C) Western blot analysis of C2CD6 and ALS2CR11B in adult mouse tissues. ACTB serves as a loading control. Note that heart lacks ACTB. (D) Localization of C2CD6 to the principal piece of wild type mouse sperm but not the *C2cd6*-null sperm. Scale bar, 25 μm.

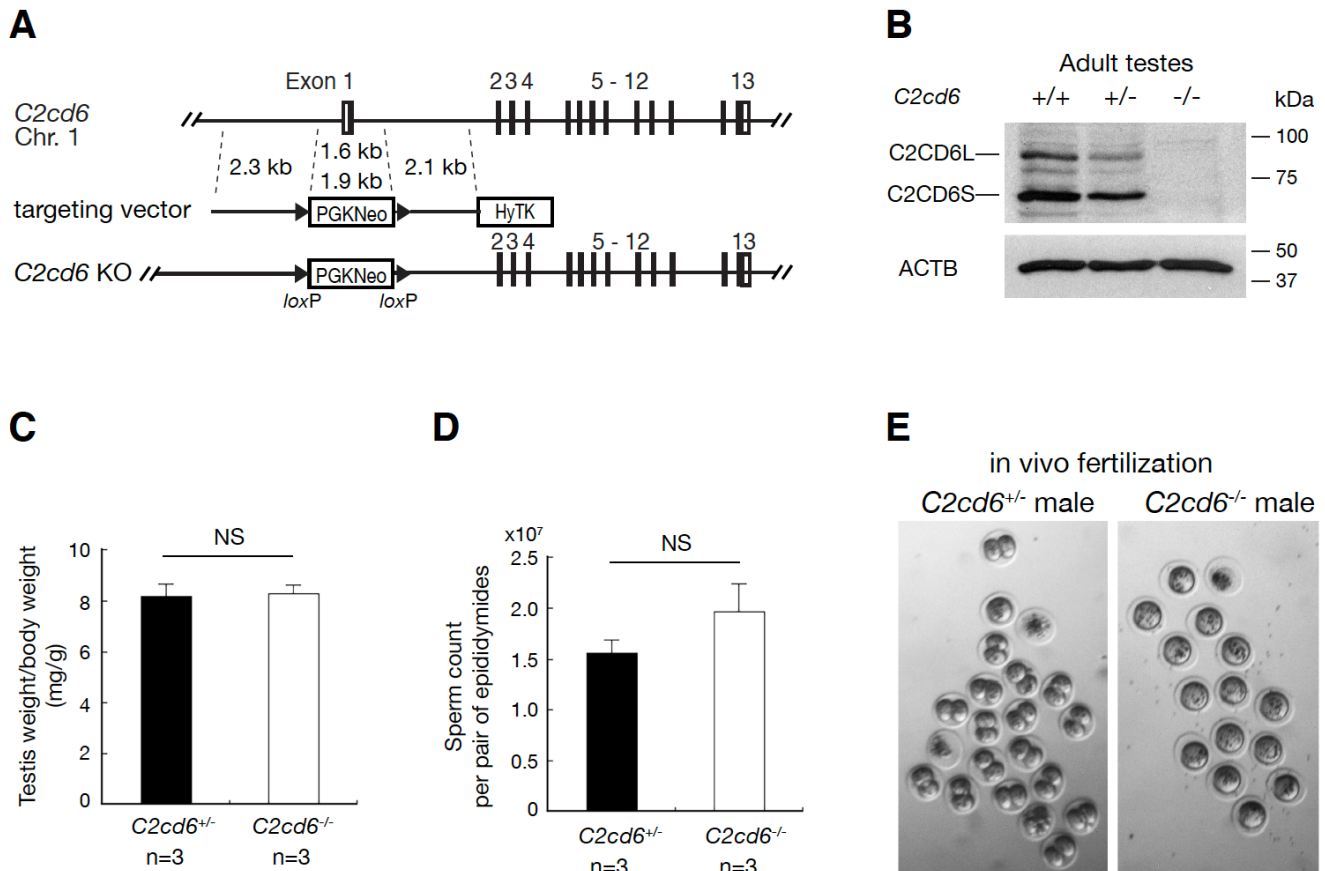


**Figure 2. C2CD6 is essential for in vivo fertilization.** (A) Targeted inactivation of the *C2cd6* gene. The 1.6-kb deleted region includes exon 1 (containing the initiating start codon) and 600-bp upstream of exon 1 (presumably the promoter region). The neomycin selection marker PGKNeo is flanked by *loxP* sites. HyTK provides negative selection by ganciclovir in ES cells. (B) Western blot analysis of C2CD6 in adult testes. ACTB serves as a loading control. (C) Testis weight normalized to bodyweight. (D) Sperm count. NS, not statistically significant. (E) In vivo fertilization assay. Embryos/unfertilized eggs were flushed from wild type females mated with either *C2cd6*<sup>+/+</sup> or *C2cd6*<sup>-/-</sup> males.

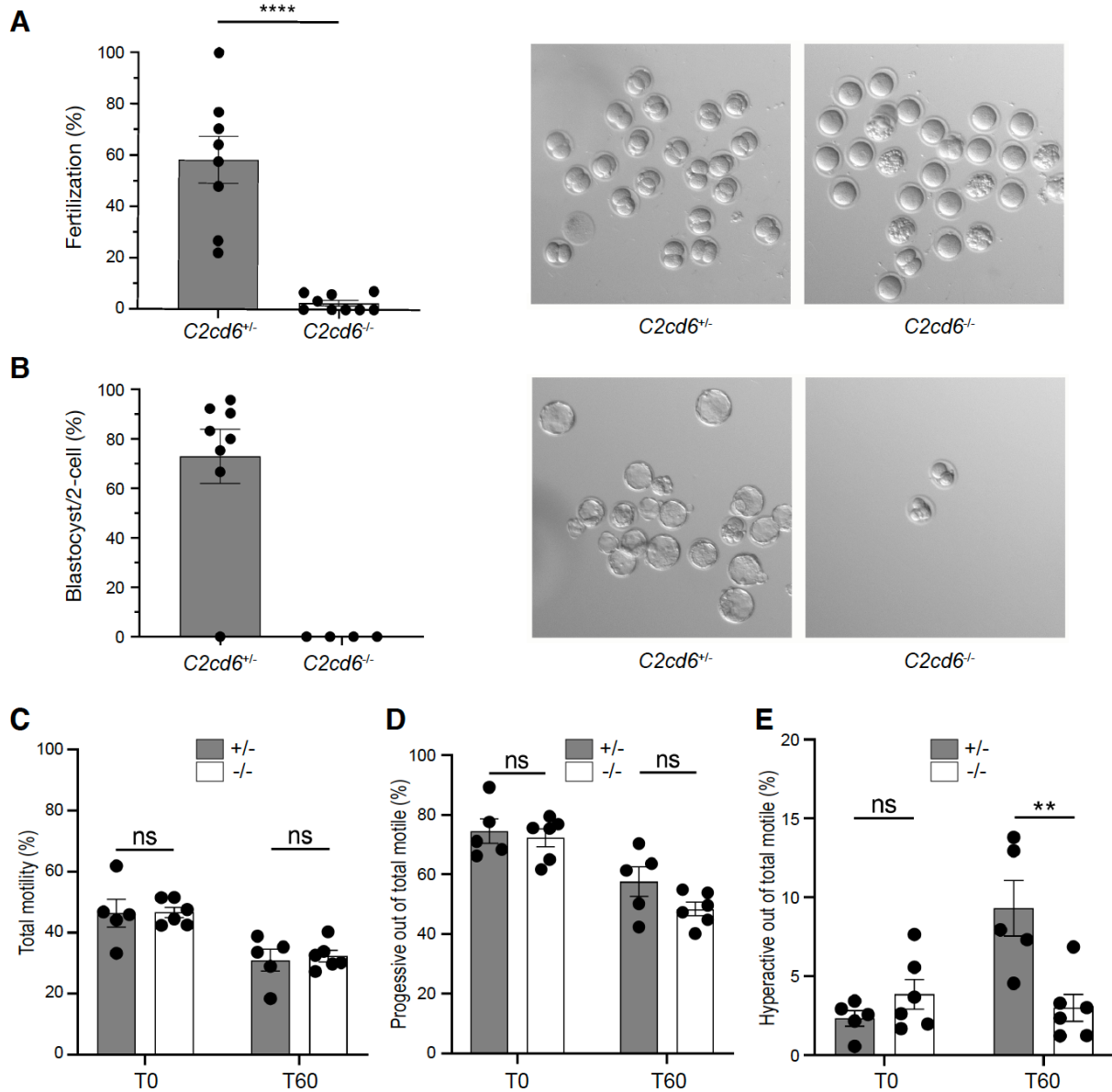


**Figure 3. C2CD6 is required for in vitro fertilization and sperm hyperactivation.** (A) In vitro fertilization. CD1 cumulus-oocyte complexes were incubated with *C2cd6<sup>+/-</sup>* or *C2cd6<sup>-/-</sup>* sperm. Fertilization rate is the percentage of oocytes inseminated that develop into 2-cell embryos after 24 hours of incubation. A representative image for each treatment is shown. \*\*\*\* $p < 0.0001$ . (B) The percentage of 2-cell embryos that develop to the blastocyst stage after culture in KSOM media. A representative image for each treatment is shown. (C) Percentage of motile sperm immediately after swim-out in TYH medium (T0) and after 60 minutes of incubation in capacitating conditions in TYH medium (T60). Sperm motility was analyzed by computer assisted sperm analysis (CASA). (D) Percentage of the motile sperm displaying progressive motility at T0 and at T60 of incubation in capacitating conditions. (E) Percentage of the motile sperm displaying hyperactive motility at T0 and at T60 of incubation in capacitating conditions. ns, not statistically significant, \*\*  $p < 0.01$ .

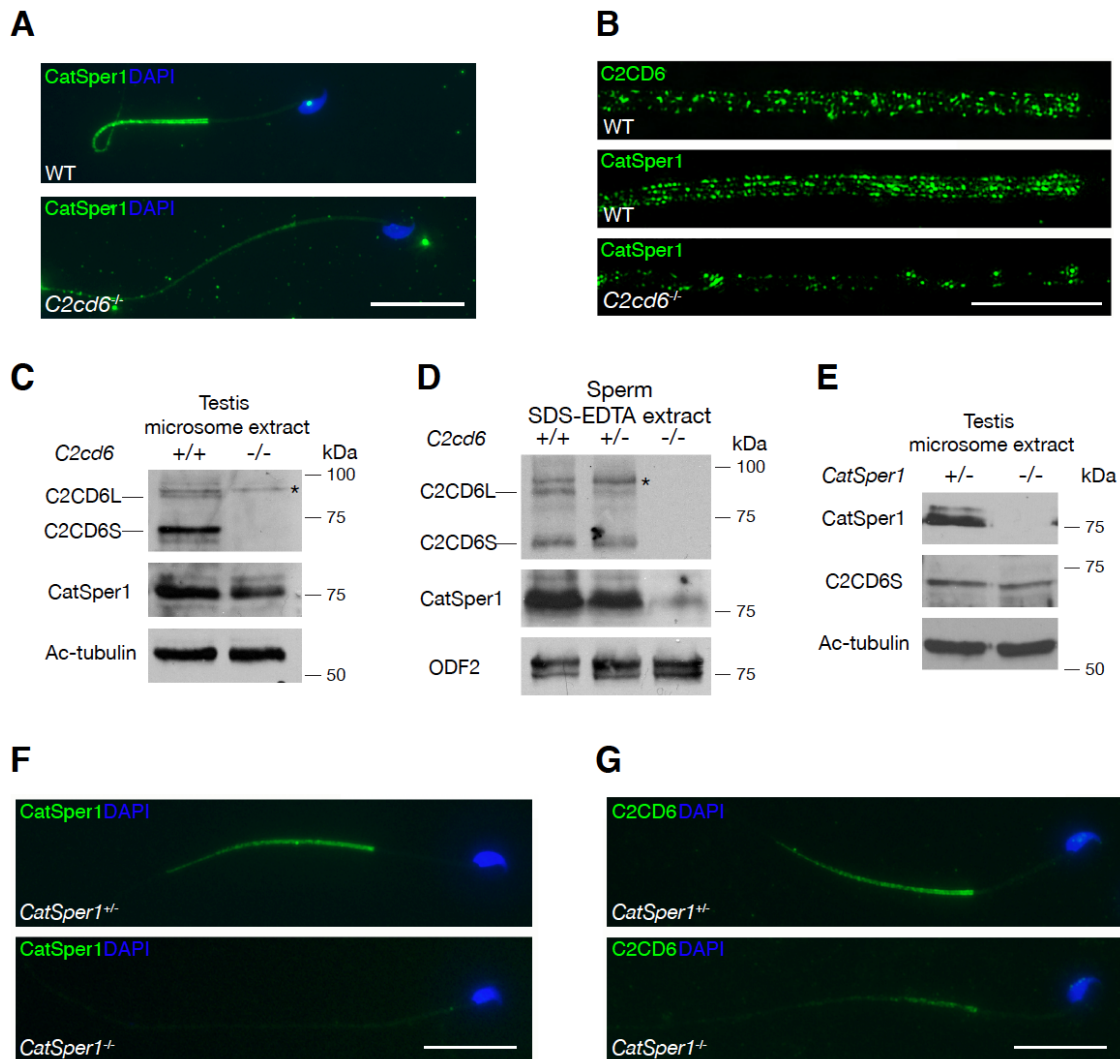


**Figure 4. C2CD6 is required for CatSper assembly in sperm flagella.** (A) Immunofluorescence analysis of CatSper1 in wild type and *C2cd6*-deficient sperm. Scale bar, 25  $\mu$ m. (B) Super-resolution localization of C2CD6 and CatSper1 in sperm. Scale bar, 5  $\mu$ m. (C) Western blot analysis of C2CD6 and CatSper1 in testis microsomes fractions. Acetylated tubulin serves as a loading control. (D) Western blot analysis of C2CD6 and CatSper1 in sperm extracts. ODF2, a component of flagellar outer dense fibers, serves as a loading control (Cao et al., 2006). (E) Immunofluorescence analysis of CatSper1 in *CatSper1*<sup>+/-</sup> and *CatSper1*<sup>-/-</sup> sperm. (F) Localization of C2CD6 in *CatSper1*<sup>+/-</sup> and *CatSper1*<sup>-/-</sup> sperm. Scale bars, 25  $\mu$ m.

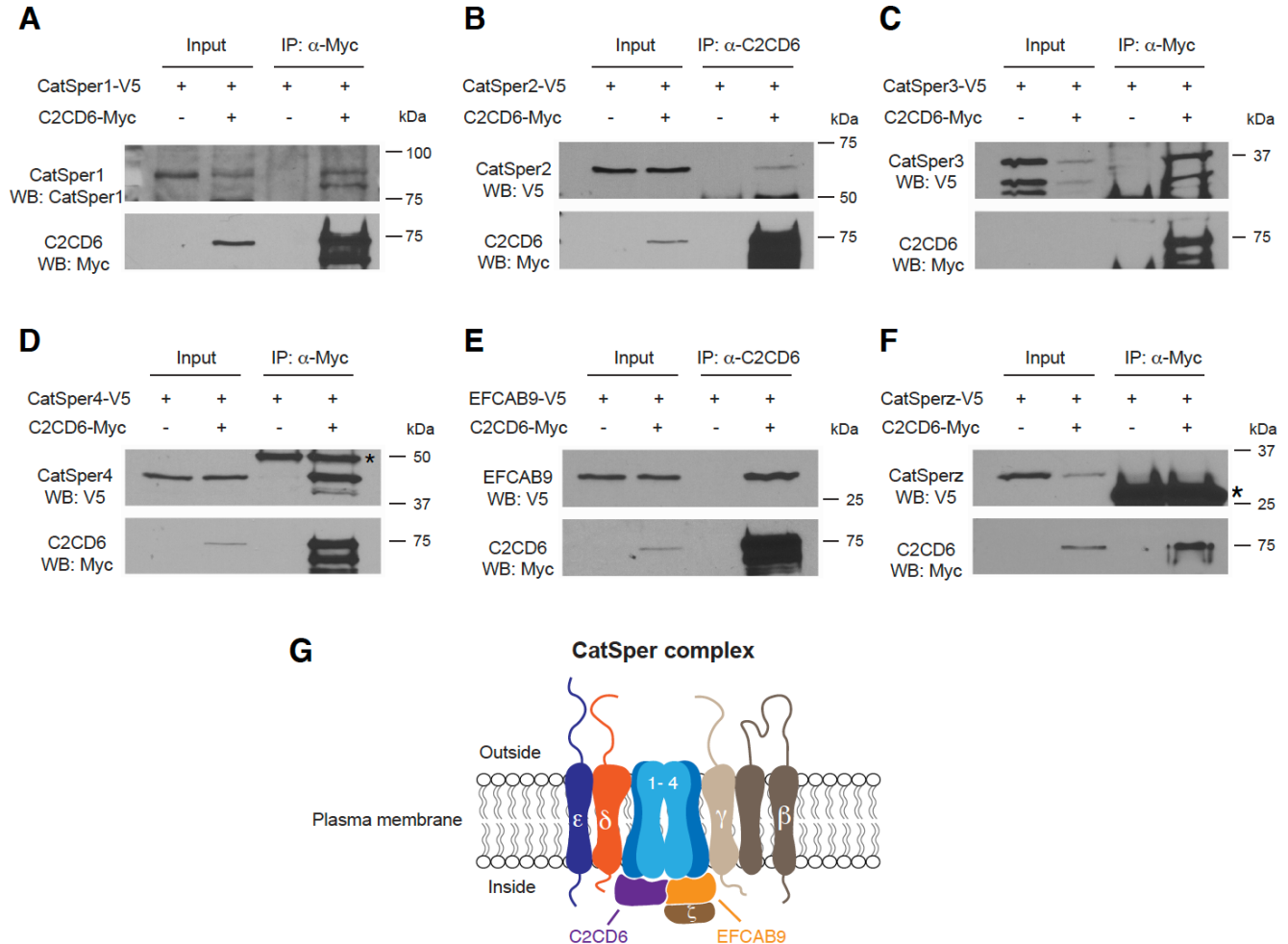


**Figure 5. C2CD6 interacts with subunits of the CatSper channel complex.** HEK293T cells were transfected with indicated expression constructs and protein extracts were used for immunoprecipitation. Coimmunoprecipitation of C2CD6 with CatSper1 (A), CatSper2 (B), CatSper3 (C), CatSper4 (D), and EFCAB9 (E). Asterisk in panel D indicates Ig heavy chain. (F) C2CD6 is not associated with CatSperz. Asterisk indicates Ig light chain. (G) A working model of the CatSper channel complex. Eleven known subunits of the CatSper channel including C2CD6 are shown. C2CD6 interacts with CatSper 1-4 and EFCAB9.